Electrodeposition of Zn-Ni Alloy from an Acid Sulphate Bath containing Ethanolamines

V. Narasimhamurthy and B.S. Sheshadri

Department of Studies in Chemistry, Central College, Banagalore University, BANGALORE - 560 001.

Electrodeposition of Zn-Ni alloy containing 10-15% Ni has been carried out from an acid sulphate bath containing ethanolamines. The effect of plating variables - such as metal ion ratio in the bath, pH, current density, temperature, stirring, concentration of ethanolamines in the bath and thickness - on the alloy composition & cathodic current density has been investigated. The phase structure and the surface morphology of electrodeposited Zn-Ni alloy (scanning electron microscopy) and hardness (on Vicker's scale) are reported.

In the recent past many efforts have been directed towards the development of high corrosion resistant steel for automotive body panels [1-4]. It has been shown that electrodeposited zinc alloys are suitable for this application [5,6]. A major development in this area focussed attention on the production of Zn-Ni alloy coatings, which show remarkable corrosion resistance properties [7,8]. These electrodeposits show low hydrogen embrittlement on the metal, so that they have been advantageously used as a substitute for cadmium coatings [9].

The electrodeposition of Zn-Ni alloy is of anomalous codeposition type as proposed by Brenner [10], i.e. under most conditions, less noble metal is deposited at the cathode preferentially to more noble metal.

The Zn-Ni alloys have been deposited from various types of baths like chloride [11-13], sulphate [14-16], sulphamate & sulphate-sulphamate [17 a & b], sulphate-chloride [7], pyrophosphate [18], ammonical [14] and cyanide baths [19].

Zinc-nickel alloy deposition from a complex bath containing more than one organic additive has led to the production of alloy with a low percentage of nickel, but found to have corrosion resistance [20]. Nitrogen containing organic compounds - specially amines - are used in plating baths for Zn-Ni alloy deposition. Review of the literature reveals the absence of comprehensive work on the electrodeposition of Zn-Ni alloy from acid sulphate bath containing ethanolamines. In this paper the effect of mono-, di- and tri- ethanolamines on the deposition of the alloy is reported.

EXPERIMENTAL

The plating bath solution were prepared using distilled water and laboratory grade chemicals. The bath solution was purified as described earlier [21]. The bath composition and operating conditions used in this study are given in Table 1.

Electrodeposition was carried out galvanostatically at 328 K under stirred conditions. A stainless steel anode was

© E.C.S.I. Bangalore

Table 1

Composition and Operating Conditions for Electro deposition of Zn - Ni Alloy Containing 10-15 % Ni

Acid Sulphate Bath in presence of Ethanolamines

Bath component	Range studied	Optimum Composition & Condition
Total metal content	-	0.2 M
$ZnSO_4$. $7H_2O$	0.04-0.12 M	0.1 M
$NiSO_4$. $7H_2O$	0.08-0.16 M	0.1 M
Triethanolamine (or) Diethanolamine (or) Monoethanolamine	0.05-0.4 M	0.1 M
Saccharin	1-6 g/l	2 g/l
$(NH_4)_2SO_4$	20-80 g/l	40 g/l
H_3BO_3	10-60 g/l	30 g/l
Sodium laurylsulphate	0.05-0.4 g/l	0.2 g/l
Temperature	25-75°C	55°C
pH	4.5-6.5	5.5
Current density	2.5-80 A.dm^{-2}	40 A.dm^{-2}
Stirring	-	normal

used as auxilary electrode. Deposited alloy was stripped in 20% HNO_3 and analyzed for metal content (hence composition of the alloy) by atomic absorption spectrometry.

Deposition potentials were recorded w.r.t SCE by using scanning potentiostat. The adhesion of the alloy deposits to the base metal was tested by a standard bending test. The porosity of the alloy deposit was determined by the ferroxyl test. The microhardness of the alloy deposits was determined on Vicker's scale.

The phase structure of the Zn-Ni alloy deposits were examined by X-ray powder diffraction (Filter CuK_{α} 30 kV, 20 mA, 4000 counts). Zn-Ni alloys were deposited upto 10 μm thick on a copper plate for X-ray analysis. Scanning electron microscopy was used to study the morphology of the alloy deposits coated over a polished copper substrate.

RESULTS AND DISCUSSION

Fig.1 shows the cathodic polarization curves for Zn-Ni alloy as well as individual metal deposition. Curve 1 is the current density - potential curve for deposition of Ni alone; the deposition potential of nickel was around -0.84 V. Curve 2 represent zinc deposition alone at a potential of -1.03 V and curve 3 is for Zn-Ni alloy deposition from the same bath solution. The deposition potential for the alloy was around -1.15V. The position of potential of

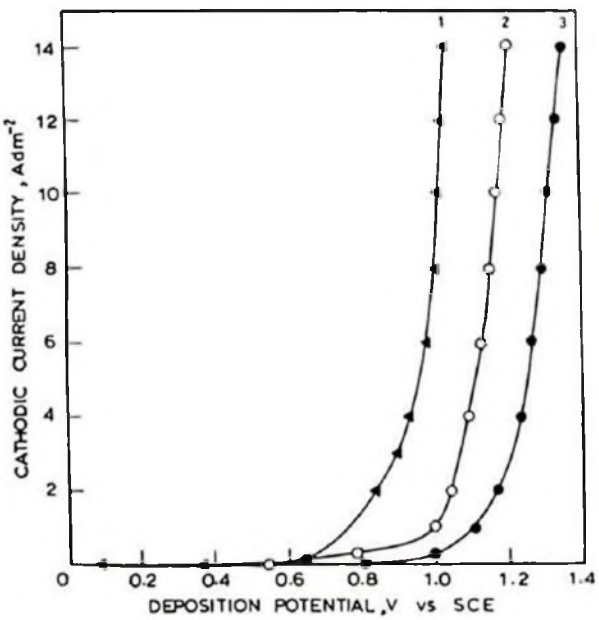


Fig.1. Cathodic Polarization Curves for the Deposition of Nickel, Zinc and Zn-Ni Alloy from an Acid Sulphate Bath
Curve 1. Deposition of nickel
Curve 2. Deposition of zinc
Curve 3. Deposition of alloy

alloy deposition curve is shown to be more negative to both nickel and zinc. These observations clearly show the reason for preferential deposition of zinc to nickel i.e. anomalous codeposition.

To study the effect of metal ion ratio in the bath on the alloy composition, zinc to nickel ratio in the bath was varied from 20:80 to 60:40. Fig.2 shows the variation of alloy composition with bath composition containing fixed concentration of ethanolamines. Under these conditions, zinc gets deposited preferentially to nickel.

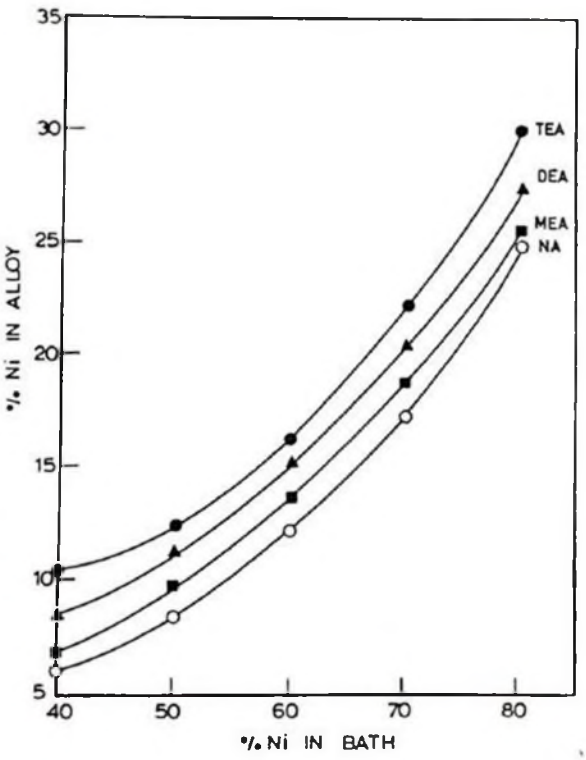


Fig.2. Dependence of % Ni in Alloy on the % Ni in the Bath
Bath Composition and Operating Conditions as in Table 1
$[Zn^{2+}]$ = 0.04 - 0.12 M;
$[Ni^{2+}]$ = 0.16 - 0.08 M;
Thickness of the deposit 4 μm;
stirred condition.

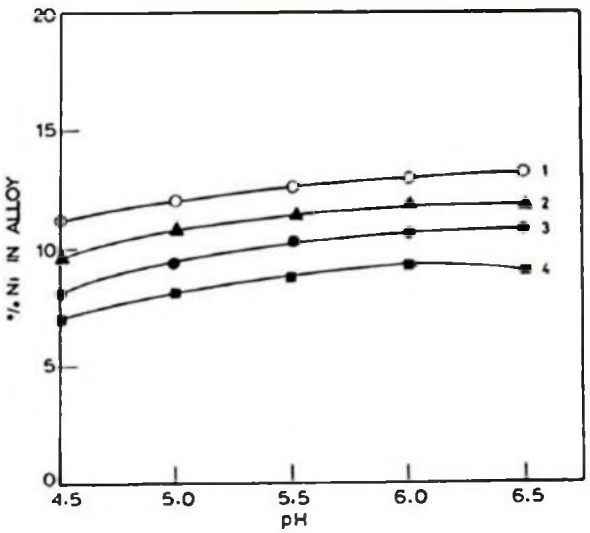


Fig.3. Variation of Alloy Composition on the pH of the Plating Bath.
Bath Composition and Operating Conditions as in Table 1
Thickness of the deposit 4 μm; stirred condition.
Curve 1: TEA. Curve 2: DEA.
Curve 3: MEA. Curve 4: NA.

A bath having higher percentage of nickel (50%) produced an alloy deposit with low percentage (12%) of nickel. This characteristic is due to preferential deposition of zinc over nickel (anomalous codeposition process). This is attributed to the formation of zinc hydroxide film at the cathode which suppresses the deposition of nickel [25].

It was observed that an increase in pH of the bath solution increased the percentage of nickel in the alloy deposit (Fig.3).

In order to study the effect of current density on the composition of Zn-Ni alloy, experiments were carried out at various current densities (5-80 $A.dm^{-2}$) using bath solutions containing constant molar ratio of Zn/Ni (50/50) and 0.1 M of mono-, di- and tri- ethanolamines at 328°K. The variation

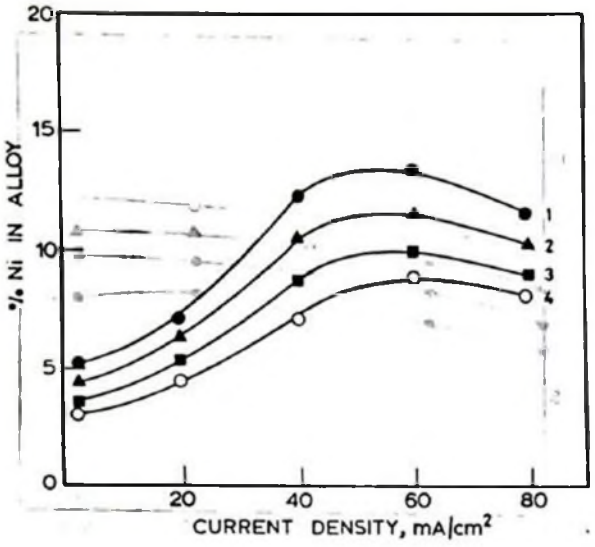


Fig.4. Dependence of Alloy Composition on Current Density.
Bath Composition and Operating Conditions as in Table 1
Current Density Range 2.5 - 80 A.dm^{-2}.
Curve 1: TEA. Curve 2: DEA.
Curve 3: MEA. Curve 4: NA

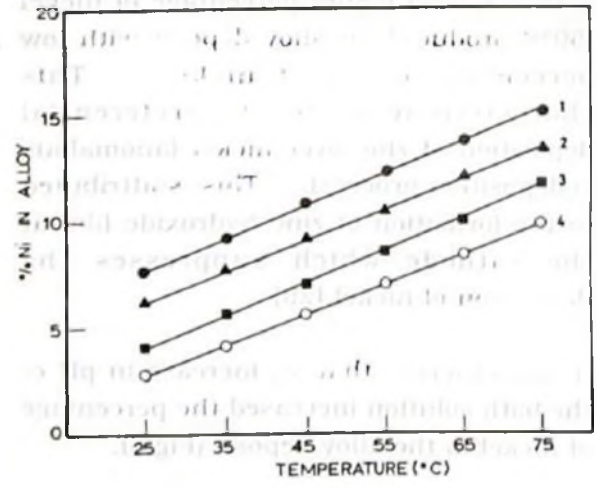


Fig.5. Variation of Alloy Composition with Temperature of the Operating Bath.
Bath Composition and Operating Conditions as in Table 1
Temperature 25 - 75°C
Curve 1: TEA. Curve 2: DEA.
Curve 3: MEA. Curve 4: NA.

in the composition of the deposited alloy with current density is shown in Fig.4. The percentage of nickel in the alloy deposit increases with current density upto 40 A.dm^{-2}. With further increase in current density, the cathode potential becomes more negative and hence the percentage of nickel shows a downward trend. This decrease in percentage of nickel with increase in current density clearly indicates diffusion controlled nature of Zn-Ni alloy deposition.

Increase in temperature of the plating bath increased the percentage of nickel in the alloy deposit (Fig.5). This is probably due to the decrease in the polarization potential of nickel (more noble metal) during alloy deposition.

Fig.6 illustrates the dependance of the percentage of nickel in the alloy on the concentration of ethanolamines in the bath. The amount of nickel in the alloy deposit increased with increase in concentration of ethanolamines, attained a maximum value at 0.2 M and then decreased slightly with further increase in the concentration of ethanolamines (>0.2 M). The formation of a loose complex with metal ions always facilitate the deposition process. In the present system, the nickel complex formed with different ethanolamines used may be active at the cathode which stimulate electrochemical discharge of nickel at higher rate. At concentrations of ethanolamines higher than 0.25 M, the nickel may form strong complex which may retard the deposition of nickel. This leads to a decrease in the percentage of nickel in the alloy deposit at higher ethanolamine concentration (Table 2).

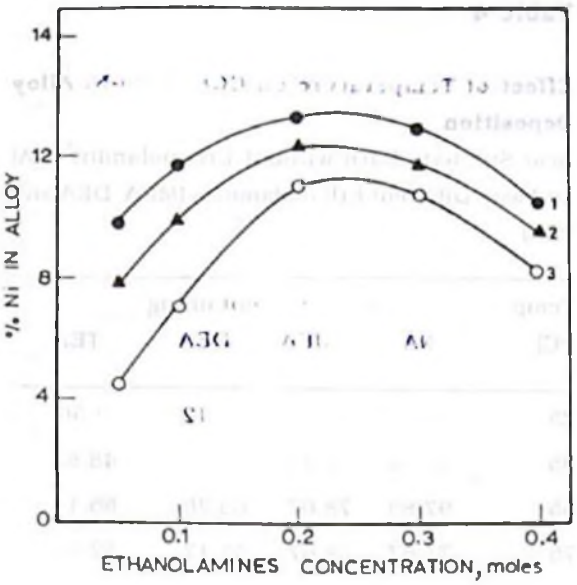


Fig.6. Dependency of Alloy Composition on Concentration of Ethanolamines
Bath composition and Operating Conditions as in Table 1.
Ethanolamine variation 0.05-0.4 M.
Curve 1: TEA. Curve 2: DEA. Curve 3: MEA.

The effect of stirring on the alloy composition was examined by carrying out experiments under stirred as well as unstirred conditions. The percentage of nickel in the alloy deposit was found to be high under stirred conditions compared to those obtained under unstirred conditions (Table 3). A significant increase in the percentage of nickel in the alloy deposit with stirring of the bath clearly indicates that deposition is under diffusion control.

Table 2

Dependance of Deposition Rate of Zn-Ni Alloy with the Concentration of Ethanolamines in the Bath

Ethanolamine concen. (M)	Deposition rate mg/cm²/sec MEA	DEA	TEA
0.0025	12.20	10.19	7.44
0.05	13.16	10.23	9.80
0.1	14.54	11.78	10.24
0.2	11.58	9.04	8.22
0.4	9.65	8.54	6.98

Table 3

Composition and Cathodic Current Efficiency (%E) of Zn-Ni Alloy

Acid sulphate bath containing ethanolamines; Temp 55°C; with and without stirring:

Parameter	CCE in Media Containing 0.1 M of Noamine	MEA	DEA	TEA
Without Stirring				
%Ni	7.51	8.82	10.50	12.33
%E	97.89	78.07	63.26	56.11
Without Stirring				
%Ni	6.33	7.67	9.48	11.14
%E	88.17	73.66	60.59	54.02

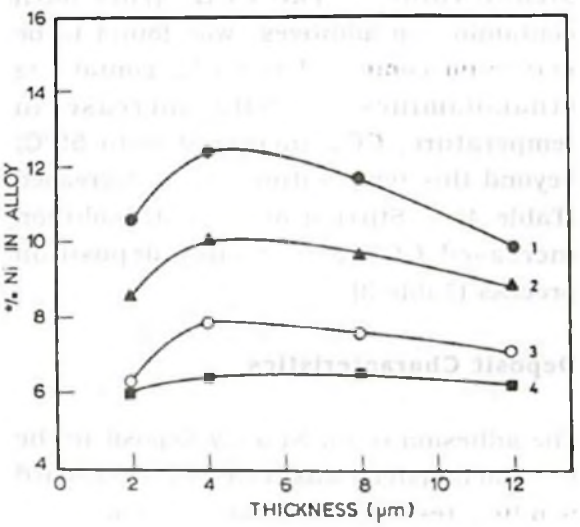


Fig.7. Variation of alloy composition with thickness of the alloy deposit.
Bath Composition and Operating Conditions as in Table 1.
Thickness variation 2-12 μm; stirred condition.
Curve 1: TEA. Curve 2: DEA.
Curve 3: MEA. Curve 4: NA.

The variation of alloy composition with its thickness is illustrated in Fig.7. The percentage of nickel in the deposit increased upto 4 μm. With further increase in deposit thickness, the percentage of nickel in the alloy deposit showed a downward trend. This dependance of alloy composition on the thickness is correlated with the concentration - time profile of the metallic ions across the cathode diffusion layer. Beyond 4 μm thickness, the cathode diffusion layer may not supply enough of nickel ions to the cathode surface and hence the decrease in the percentage of nickel in the alloy deposit.

The cathodic current efficiencies (CCE) were calculated for the Zn-Ni alloy deposition under each set of experimental conditions. Fig.8 shows the dependance of CCE on current density. With increase in current density, the CCE increased and attains a steady value. The CCE from bath containing no additives was found to be maximum compared to baths containing ethanolamines. With increase in temperature, CCE increased upto 55°C: beyond this temperature, CCE decreased (Table 4). Stirring of the bath solution increased CCE of the alloy deposition process (Table 3).

Deposit Characteristics

The adhesion of Zn-Ni alloy deposit to the base metal (steel) was tested by a standard bending test. Alloy samples coated to different thickness (2-12 μm) on steel (1x4 sq. inch) were subjected to bending tests. The alloy coatings did not develop any visual cracks even after 180° bending. This shows a good adhesion of the alloy deposits to the steel surface.

Table 4

Effect of Temperature on CCE of Zn-Ni Alloy Deposition

Acid Sulphate Bath without Ethanolamine (NA) and with Different Ethanolamines (MEA, DEA and TEA)

Temp (°C)	CCE in media containing NA	MEA	DEA	TEA
25	19.10	17.87	15.12	9.56
35	76.56	61.11	51.96	48.82
55	97.89	78.07	63.26	56.11
75	71.67	58.67	52.17	52.01

Porosity tests were carried out on alloy coated to 2-12 μm thickness on steel panels (3x3 sq. inch). A filter paper soaked in 1% $K_3Fe(CN)_6$ solution was placed on alloy

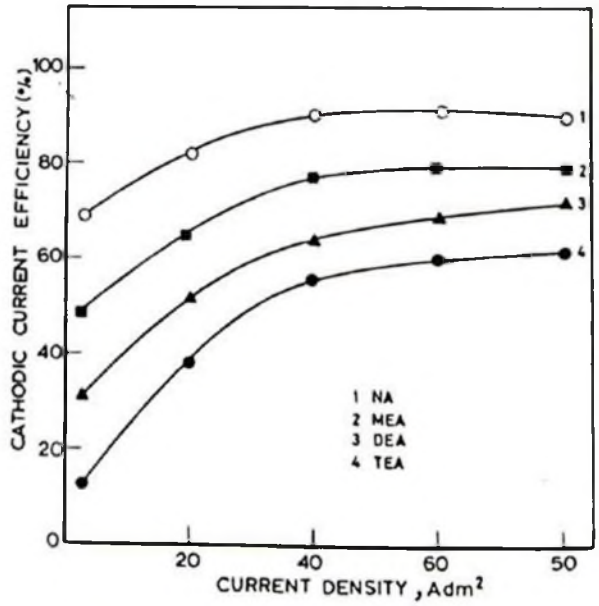


Fig.8. Dependence of Cathodic Current Efficiency on Current Density.
Curve 1: NA, Curve 2: MEA,
Curve 3: DEA, Curve 4; TEA.

coated steel panels. The number of blue spots appearing on the filter paper with time was a measure of porosity of the deposit. The alloy deposits were pore free at thickness > 4 μm.

The microhardness of Zn-Ni alloy (10 μm thick deposit) specimens was determined. The hardness of the alloy deposits increased with increase in nickel content in the alloy (Table 5).

The static potential values for zinc and zinc-nickel alloy were measured w.r.t. SCE in 3.5% NaCl solution (Table 5). Static potnetial for alloy was found to be less noble to steel and more noble to zinc. This shows that Zn-Ni alloy coatings protect steel more efficiently than zinc coatings.

Table 5

Effect of Nickel Content in the Zn-Ni Alloy on Microhardness and on Static Potentials

% Ni in alloy	microhardness in VHN (load - 50 gm)	Static potential in mV *vs* SCE in 3.5% NaCl
0	120	-1060
10	300	-1050
15	330	-1043
20	370	-1028
25	450	-1010
Mild Steel	-	- 580

The phase structure of electrodeposited Zn-Ni alloy from an acid sulphate bath containing ethanolamines was studied by X-ray powder diffraction. Fig.9 shows the relationship between the phase and the percentage of nickel in the alloy deposit. The phase diagram of Zn-Ni alloy reveals the presence of (η) Hexogonal, (δ) F.C.C., (γ) B.C.C. and (α) B.C.C. intermetallic phases. Low zinc containing alloy shows a solid solution of zinc in nickel i.e. α-phase, whereas zinc rich alloy deposits showed

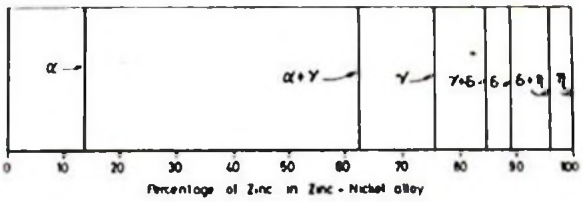


Fig.9. Relationship between phase and percentage of zinc in the Zn-Ni alloy electroplated from an acid sulphate bath.

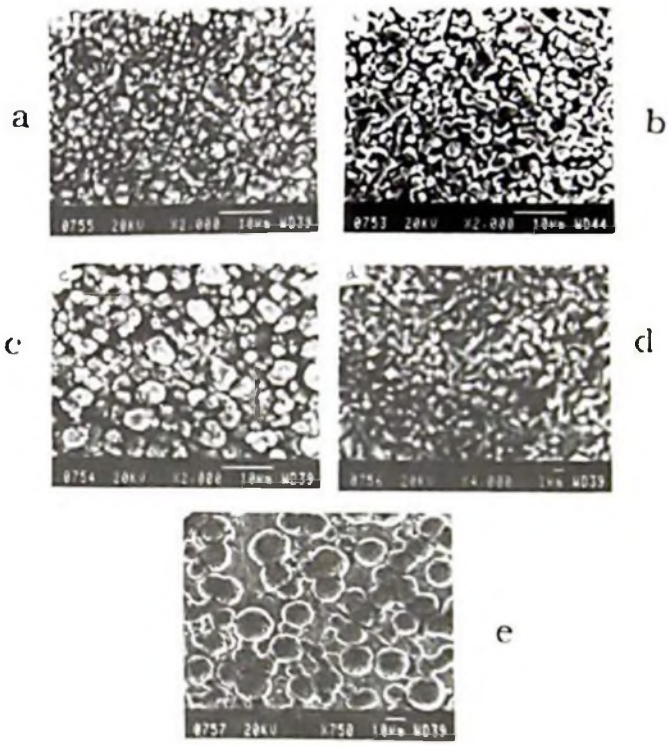


Fig.10. Scanning electron micrographs of Zn-Ni alloy deposits obtained from an acid sulphate bath containing various ethanolamines. x = 330.
a. bath containing no amines
CD = 40 A.dm $^{-2}$
b. bath containing monoethanolamine.
CD = 40 A.dm $^{-2}$
c. bath containing diethanolamine.
CD = 40 A.dm $^{-2}$
d. bath containing trienanolamine.
CD = 20 A.dm $^{-2}$
e. bath containing trienanolamine
CD = 40 A.dm $^{-2}$

intermetallic phases η, δ and γ. This agrees with the obsrvations of earlier workers [12.17b]. However, the presence of β and γ were not observed in the present case. Thus electrodeposited Zn-Ni alloys have co-existing metastable and intermetallic phases over a wide range of composition: η (89-100% Zn), γ (13.5 - 84.5% Zn), δ (75.5 - 89% Zn) and α (0.62.5% Zn).

The surface morphology of Zn-Ni alloy deposits were examined under scanning electron microscope. Fig.10 shows the morphology of Zn-Ni alloy deposits obtained at 40 $A.dm^{-2}$ from an acid sulphate bath containing various ethanolamines. The morphology was found to vary for different amines. Finer grained deposits were obtained from bath containing triethanolamine at 20 $A.dm^{-2}$.

CONCLUSION

Electrodeposition of Zn-Ni alloy having 10-15% Ni from an acid sulphate bath containing ethanolamines follows anomalous codeposition. The deposition potential of alloy is less noble to both zinc and nickel deposition. A bath having high nickel content produces an alloy with low nickel content. Increase in bath pH, current density, temperature and stirring increases the percentage of nickel in the alloy deposit. With increase in thickness of the alloy deposit, the percentage of nickel increases, reaches a maximum and then decreases with further increase in thickness. The cathodic current efficiency is dependant on current density, temperature and stirring of the bath. Intermetallic phases appear in electrodeposited Zn-Ni alloy. Hardness of the alloy increases with increase in nickel content of the alloy. Fine grained deposits are obtained morphologically for Zn-Ni alloy containing 15% Ni from baths containing various ethanolamines.

REFERENCES

1. T. Watanabe, M. Omura, T. Honma and T. Adaniya, *SAE, Tech. pap. series no. 820424*, **Detriot, Michigan** (1982).
2. A. Shibuya, T. Kurimoto, K. Korekawa and K. Noji, *Tetsu-to-Hagane*, **66** (1980) 771.
3. R. Noumi, H. Nagasaki, Y. Foboh and A. Shibuya, *SEA, Tech. pap. Series No. 820332*, **Detroit, Michigan** (1982).
4. T. Kurimoto, Y. Foboh, H. Oishi, K. Yanagawa and R. Noumi, *SAE, Tech. pap. Series No. 831837*, **Warrendale, Pennsylvania** (1983).
5. K. Ariga and K. Kanada, *Tetsu-to-Hagane*, **66** (1980) 797.
6. T. Fukuzuka, K. Jajiawara and K. Miki, *Tetsu-to-Hagane*, **66** (1980) 807.
7. V. Raman, M. Pushpavanam, S. Jayakrishnan and B.A. Shenoi, *Met. Finish.*, **81** (1983) 85.
8. D.E. Hall, *Plat. Surf. Finish.*, **71** (1983) 59.
9. G.F. Hsu, *Plat. Surf. Finish.*, **71** (1984) 52.
10. A. Brenner, *Electrodeposition of Alloys, Vols. I and II*, **Academic Press, New York and London** (1963).
11. E.J. Roehl, *U.S. Patent 3, 420.754* (1969); **U.S. Patent 3, 558, 442** (1971).
12. B. Lustman, *Trans. Electrochem. Soc.* **84** (1943) 363.
13. A. Abibsi, J.K. Dennis and N.R. Short, *Trans. I.M.F.*, **69** (1991) 145.
14. S.R. Rajagopalan, *Met. Finish.*, **70** (1972) 52.
15. E.P. Schouch *et al.*, *J.Am. Chem. Soc.*, **29** (1907) 314.
16. S. Glasstone, *J. Chem. Soc.*, **130** (1927) 641.
17. J.W. Dini and H.R. Johnson, *Met. Finish.*, (a) **78** (1980) 45; (b) **77** (1979) 31.
18. T.L. Rama Char and S.K. Pantkkar, Electroplating and Metal *Finishing*, **13** (1960) 405.
19. L. Domnikov, *Met. Finish.*, **63** (1965) 63.
20. R. Alabalt, E. Gomez, C. Muller, J. Pregonas, M. Sarret and E. Valle's, (a) *J.Appl. Electrochem.*, **22** (1992) 657; (b) *J.Appl. Electrochem.*, **20** (1990) 635; (c) *Met. Finish.*, **90** (1992) 87.
21. K. Higashi, H. Fukushima, T. Urokawa, T. Adaniya and K. Matsudo, *J. Electrochem. Soc.*, **128** (1981) 2081.